

5-2015

Investigation of the interaction between graphene oxide and a biopolymer surface

Pei Pang
College of William and Mary

Follow this and additional works at: <https://scholarworks.wm.edu/honorsthesis>



Part of the [Biology and Biomimetic Materials Commons](#), [Biomaterials Commons](#), [Other Materials Science and Engineering Commons](#), and the [Polymer and Organic Materials Commons](#)

Recommended Citation

Pang, Pei, "Investigation of the interaction between graphene oxide and a biopolymer surface" (2015). *Undergraduate Honors Theses*. Paper 235.
<https://scholarworks.wm.edu/honorsthesis/235>

This Honors Thesis is brought to you for free and open access by the Theses, Dissertations, & Master Projects at W&M ScholarWorks. It has been accepted for inclusion in Undergraduate Honors Theses by an authorized administrator of W&M ScholarWorks. For more information, please contact scholarworks@wm.edu.

**Investigation of the interaction between graphene oxide and a
biopolymer surface**

A thesis submitted in partial fulfillment of the requirement
for the degree of Bachelor of Science in Chemistry and of the requirement for a minor in Applied
Sciences from The College of William and Mary

by

Pei Pang
Pei Pang

Accepted for Honors

(Honors)

Hannes Schniepp

Hannes Schniepp, Director

John Poutsma

John Poutsma

David Kranbuehl

David Kranbuehl

Williamsburg, VA
May 6, 2015

APPLIED SCIENCE DEPARTMENT

THE COLLEGE OF WILLIAM & MARY

**Synthesis of a graphene oxide and
Loxosceles spider silk nanocomposite**

By Pei Pang

This material is based upon work supported by the National Science Foundation under Grant
No. DMR-1352542

Advisor: Hannes Schniepp

Table of Contents

Abstract	- 1 -
Introduction	- 2 -
Loxosceles spider silk.....	- 2 -
Graphene and Graphene Oxide.....	- 2 -
Graphene oxide- <i>Loxosceles</i> spider silk nanocomposite.....	- 3 -
Synthesis methods on glass.....	- 3 -
Synthesis methods on PDMS.....	- 3 -
Materials and Methods	- 5 -
Materials.....	- 5 -
Spin-coating.....	- 5 -
Acid-Incubation.....	- 5 -
Natural drying of GO solution.....	- 6 -
Imaging methods.....	- 6 -
Results and discussion	- 10 -
Spin-coating method.....	- 11 -
Natural drying of GO solution.....	- 14 -
Acid-incubation.....	- 19 -
Future perspectives.....	- 23 -
Conclusion	- 24 -
Acknowledgements	- 25 -
Reference	- 26 -

Table of Figures

Figure 1. Diagram of the elastic cantilever and the laser signaling system	- 7 -
Figure 2. Schematic diagram of how AFM probe maps the surface topography.....	- 8 -
Figure 3. Schematic diagram of twisting of cantilever.	- 9 -
Figure 4. Schematic diagram of FMM.....	- 10 -
Figure 5. Contact topography image of a selected area on the spin-coating sample	- 11 -
Figure 6. The cross-section analysis of the cross-section in Figure 5.....	- 12 -
Figure 7. LFM images of the selected area on the spin-coating sample.....	- 12 -
Figure 8. FMM image of the selected area on the spin-coating sample	- 13 -
Figure 9. Contact topography image of a selected area on the natural drying sample.	- 15 -
Figure 10. Contact topography image of a selected area on the natural drying sample	- 15 -
Figure 11. Cross-section analysis of cross-section 1 in Figure 9.....	- 16 -
Figure 12. Cross-section analysis of cross-section 2 in Figure 9.....	- 16 -
Figure 13. Cross-section analysis of cross-section 3 in Figure 9.....	- 17 -
Figure 14. LFM images of the selected sample area on the natural drying sample.....	- 17 -
Figure 15. FMM phase image of the selected sample area on the natural drying sample. -	- 18 -
Figure 16. Illustration of the Coffee-ring effect.....	- 19 -
Figure 17. Contact topography image of a selected area of the acid-incubation sample... -	- 20 -
Figure 18. Contact topography image of a selected area of acid-incubation sample..... -	- 20 -
Figure 19. Cross-section analysis of cross-section 1 in Figure 18.....	- 21 -
Figure 20. Cross-section analysis of cross-section 2 in Figure 18.....	- 21 -
Figure 21. Cross-section analysis of cross-section 3 in Figure 18.....	- 22 -
Figure 22. FMM phase image of the selected area on the acid-incubation sample.	- 22 -

Abstract

Graphene oxide and the silk of the *Loxosceles* spider are among the most exquisite materials in the world. Graphene oxide (GO) is exceptionally strong and light. The silk of the *Loxosceles* (brown recluse) spider is as strong and tough as any spider silk, yet features a unique, flat morphology closely resembling a polymer thin film with a thickness of about 50 nm. The combination of these two materials, then, can yield a novel nanocomposite. This novel material has the potential to possess a combination of outstanding properties. It would be thin, lightweight, strong, electronically conductive, and biocompatible. Therefore, this material can have many potential applications in various fields, such as biocompatible coatings and body implants. In this project, we report a study of three synthesis methods of this novel graphene oxide-*Loxosceles* spider silk nanocomposite.

Introduction

Loxosceles spider silk

The silk of the *Loxosceles* (brown recluse) spider is a fascinating material. It has a Young's Modulus of 21 ± 6 GPa and a maximum extensibility of 25% to 30%, making it among the strongest and toughest of all silks (1). On the other hand, *Loxosceles* spider silk also features a unique ribbon-like morphology that closely resembles a thin film with the thickness of around 50 nm (1, 2). As a result, this type of silk can be regarded as a bio-polymer thin film with high elasticity and strength, implying great potential as a polymer matrix material for nanocomposites.

Graphene and Graphene Oxide

Graphene is a single layer of sp^2 hybridized carbon atoms in a hexagon lattice (3). Due to its special geometry structure, graphene possesses outstanding mechanical properties. Single-layered graphene has a mechanical strength of up to 130 GPa and a Young's Modulus of 1200 GPa; these values are among the highest of all materials (3-5). In addition, graphene also has relatively high electrical and thermal conductivity. Because of these exceptional properties, graphene has been considered a promising filler material to reinforce polymer matrices. However, the sp^2 hybridization of graphene also brings chemical stability to the material, reducing its ability to form strong interfacial adhesion with polymer matrices (6, 7). Additionally, graphene is hydrophobic (7). As a result, it is difficult to disperse graphene in water. This creates technical difficulties in transferring graphene to polymer matrices (3, 7, 8). Graphene oxide (GO) is a material that addresses these two challenges. GO is functionalized graphene with functional groups like epoxy, hydroxyl, and carbonyl group on the graphene surface (8). The structure of GO closely resembles that of graphene, yet GO generally has reduced mechanical properties: its typical strength is 120 MPa and Young's modulus is 200 GPa. The reduction in mechanical properties is possibly caused by the disruption of sp^2 hybridization (4). Nevertheless, the addition of functional groups renders GO hydrophilic,

making it dispersible in water (3, 5-8). The functional groups can also form both covalent and non-covalent linkages with the polymer matrix, producing relatively strong interfacial adhesion between GO and polymer matrices.

Graphene oxide- *Loxosceles* spider silk nanocomposite

Since *Loxosceles* spider silk can be considered a bio-polymer thin film, graphene oxide (GO) can be added onto the silk surface to produce a novel type of graphene oxide-*Loxosceles* spider silk nanocomposite. This material would be thin, lightweight, strong, electronically conductive, and biocompatible. It therefore suggests many potential applications, such as biocompatible coating for medical devices, artificial organs, and body implants.

In this project, we study three synthesis attempts of this novel graphene oxide-*Loxosceles* spider silk nanocomposite on two substrates—glass and polydimethylsiloxane (PDMS).

Synthesis methods on glass

Due to the variation in surface chemistry of glass and PDMS, different synthesis methods of the GO-*Loxosceles* silk nanocomposite are adopted (9, 10). On glass substrate, we utilize spin-coating to produce the novel nanocomposite. Spin-coating is widely used to deposit uniform thin film to a flat substrate (11). It involves the use of a high-speed spinner to create strong centrifugal forces and high surface tension that spread a thin film solution evenly over a flat substrate. The solvent of the thin film solution will evaporate during the spin-coating process, leaving a uniform coating of thin film over the flat substrate. Since GO is a structural analog to graphene, it can be regarded as a thin film. In the meantime, the *Loxosceles* spider silk serves as the flat substrate.

Synthesis methods on PDMS

The surface of the polymer PDMS is hydrophobic (10). Therefore, the spin-coating method is not viable on PDMS because the aqueous GO solution is spun away from hydrophobic surface during the spinning process. Nevertheless, we have developed two production methods

of depositing the nanocomposite on PMDS—natural drying of GO solution and acid-incubation. In the natural drying method, we covered *Loxosceles* silk with GO aqueous dispersion solution and let the solution dry naturally in a clean desiccator. During the drying process, as the solvent evaporates, the GO flakes deposit on the silk surface. However, this method introduces unwanted contaminants onto the silk surface and the deposition of GO flakes is not be uniform.

The other method we used to synthesize the GO-*Loxosceles* silk nanocomposite on PDMS is acid-incubation. In this method, we prepared a GO solution of pH 3.3, which is lower than the isoelectric point of spider silk fibroin (12). We then covered the silk surface with the GO solution and let it incubate under a humid environment for two hours. By doing so, we introduce a strong electrostatic attraction between the positively charged silk and negatively charged GO.

Materials and Methods

Materials

GO stock solution was obtained from Professor Kranbuehl's lab with a concentration of 0.19 mg/mL. The stock solution was then diluted to 0.02 mg/mL with water purified by the Direct-Q® 3 Water Purification System. To ensure homogenous dispersion of GO and avoid aggregation of GO flakes, we enacted a 30-minute sonication in a Fisher Scientific™ Digital Ultrasonic Cleaner. Samples of *Loxosceles* spider silk were collected from the webs of *Loxosceles* spiders raised in our lab and applied to pre-cleaned substrate.

For substrates, we used Gold Seal™ Cover Glasses for glass substrate. The cover glasses were cleaned in Fisher Scientific™ Digital Ultrasonic Cleaners for 30 minutes to ensure atomic-level cleanness. The PDMS sample was prepared using a Dow Corning Sylgard 184 Silicone Elastomer kit.

Spin-coating

Before spin-coating, 5 to 10 μ l of the 0.02 mg/mL aqueous GO dispersion solution was applied to a selected flat section of *Loxosceles* silk applied on glass. The sample then was spin-coated with a rate of 3000 rounds per minute (RPM) for 3 minutes using Laurell® WS-450-6NPP spin-coater.

Acid-Incubation

In the acid incubation method, GO solution was prepared by diluting the stock GO solution (0.19 mg/mL) with hydrosulfuric acid solution to adjust the pH value to 3.3 and the solution concentration to 0.02 mg/mL. After applying *Loxosceles* silk on PDMS, we added 10-20 μ l of the acidified GO solution to cover a selected flat section of *Loxosceles* silk applied on PDMS substrate. The sample was then placed under a humid environment for 2 hours. After incubation, we spin-coated the sample at 3000 RPM for 3 minutes to remove the remaining solution.

Natural drying of GO solution

In the natural drying of GO solution, 20-30 μl of 0.02 mg/mL GO aqueous solution was applied to a selected flat section of *Loxosceles* silk applied on PDMS. The sample was then put in a desiccator overnight to evaporate all solvents.

Imaging methods

Since the sizes of both *Loxosceles* spider silk and GO are on a nanoscale, a special imaging method with nanoscale resolution is required. In this project, we used Atomic Force Microscopy (AFM) as our major imaging tool. AFM uses a special probe to scan over a certain surface area (13). The probe is composed of an elastic cantilever with a sharp tip at its point. A laser beam is directed onto the cantilever and reflects onto a photodiode detector. When the probe approaches the sample surface, the interaction between the tip and the sample causes the elastic cantilever to bend. The bending then shifts the laser beam, leading to a change of laser signal to the photodiode detector (Fig. 1).

To maintain a constant tip-sample interaction, the probe is attached to a piezoelectric actuator. The actuator uses the photodiode signal to adjust the tip-sample distance so that a fixed interaction between the tip and the sample are maintained. By doing so, the AFM is capable of mapping the topography of the scanned sample surface (Fig. 2).

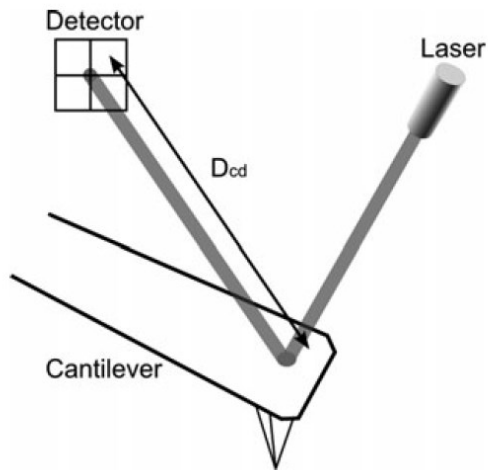


Figure 1. Diagram of the elastic cantilever and the laser signaling system. The D_{cd} is the detector-cantilever distance. D_{cd} is relatively large compared to the length of the cantilever; thus, a small bending of the cantilever results in a relatively large change in the spot of laser beam at the detector. Adapted from Eaton and West. Reference 13.

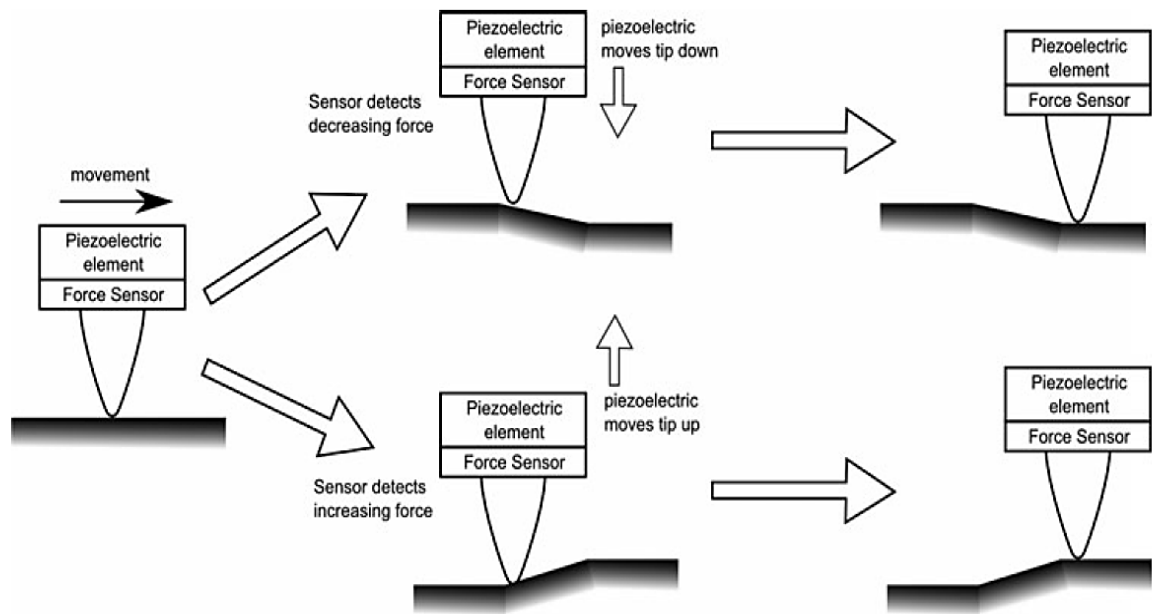


Figure 2. Schematic diagram of how AFM probe maps the surface topography. Adapted from Eaton and West. Reference 13.

In our lab, we most frequently use two basic AFM topography imaging modes—contact mode and tapping mode. In contact mode, the tip is in direct contact with the scanning sample. The force between the tip and the sample will bend the cantilever, creating a change in laser spot at the detector. However, the direct contact between the tip and the sample can damage the sample surface, especially, in biological samples (14). The tapping mode is an alternative that avoids sample damage. In tapping mode, instead of being directly in contact with the sample, the probe is oscillating at its resonance frequency. The oscillating tip is kept at an intermittent tip-sample distance. The piezoelectric actuator then will adjust the probe’s position to maintain a constant oscillating amplitude.

In our project, single layer GO has a thickness of less than 5 nm, which is close to the surface roughness of *Loxosceles* spider silk. Therefore, regular topography AFM imaging methods might be unable to show GO flakes. To solve this problem, we employed three other, more

specialized AFM imaging modes—lateral force mode (LFM), phase imaging mode, and force modulation mode (FMM).

Lateral force mode (LFM) is an AFM imaging mode that maps the frictional force between the tip and the sample. It is also a sub-mode of contact mode. As the tip moves horizontally across the sample surface, it will create friction with the sample, leading to a twist in the cantilever and a horizontal shift in the laser spot at the detector. Hence, we are able to map the variation in friction over the sample surface (Fig. 3). Variation in tip-sample friction is caused by many factors, such as surface smoothness and material stiffness.

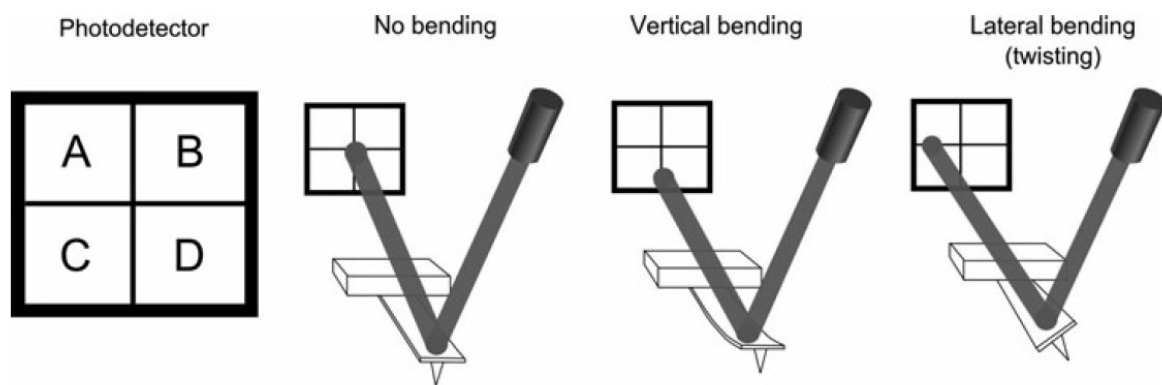


Figure 3. Schematic diagram of twisting of cantilever. Adapted from Eaton and West. Reference 13.

Another important imaging mode used in this project is force modulation mode (FMM), which maps the stiffness distribution of a surface. In this mode, the AFM probe is oscillating at a given frequency of several kHz and is in direct contact with the sample surface. The oscillation amplitude of the tip increases as the stiffness of material increases. Therefore, we map the stiffness difference of the sample surface. As softer materials lead to lower vibration amplitudes, they will show up as darker region on the FMM images (The schematic diagram of FMM mechanism is shown in Figure 4).

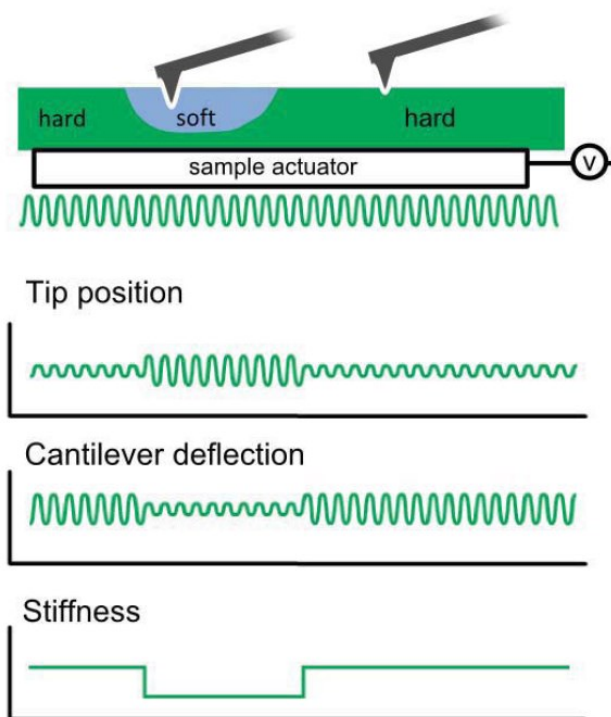


Figure 4. Schematic diagram of FMM. On softer materials, the vibration amplitude of the tip is lower than that on hard materials. Adapted from Cai. Reference 14.

One more important imaging mode is FMM phase imaging. FMM phase imaging is a sub-mode of tapping mode and also force modulation mode. In both modes, the probe is oscillating at a fixed frequency. When scanning across a surface area, the differences in surface character, such as stiffness and surface chemistry, will lead to variation in tip-sample interaction. Such variation shifts the phase of oscillation, leading to a contrast between regions with different material characteristics. In FMM, a brighter region in the images corresponds to a stiffer material. However, such correspondence does not exist in FMM phase imaging and LFM imaging, as both imaging modes can only distinguish different materials without illustrating their properties.

Results and discussion

The AFM images were acquired using the NT-MDT model NTEGRA Prima. AFM images were processed using Nova-scan, Gwyddion, and Inkscape software.

Spin-coating method

The spin-coated sample was scanned with contact topography mode, LFM mode, and FMM modes (Figs. 5–8).

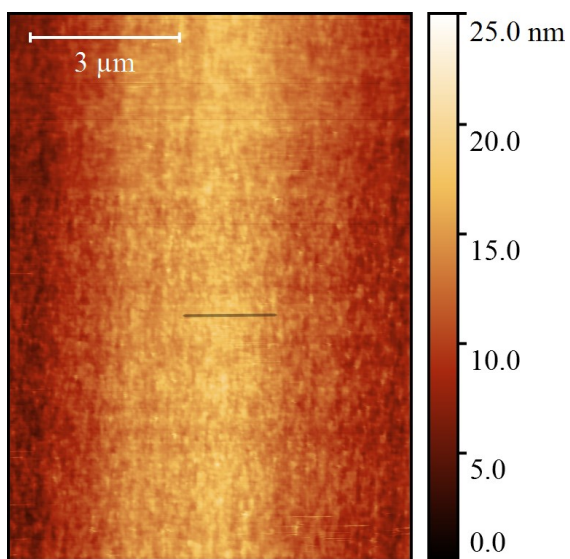


Figure 5. Contact topography image of a selected area on the spin-coating sample. The black line in the middle of the image is the selected cross section that is analyzed in Figure 6.

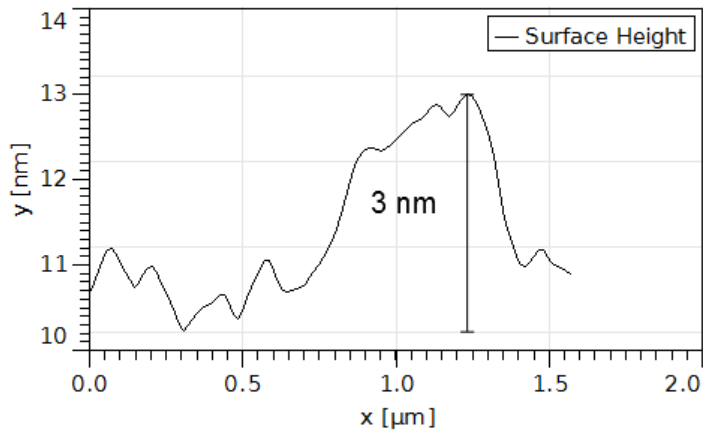


Figure 6. The cross-section from Figure 5. The height value is rounded to the nearest whole number.

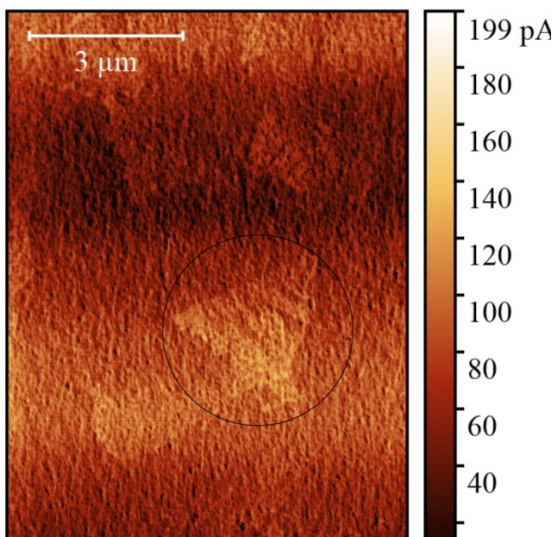


Figure 7. LFM images of the selected sample area. The circled triangular shape object is a GO flake.

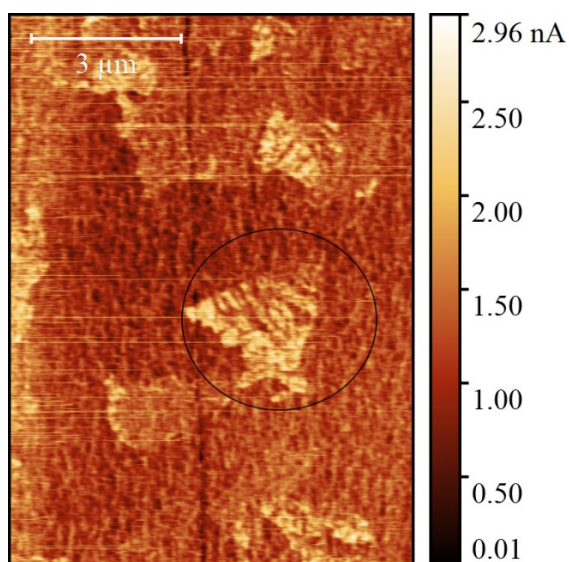


Figure 8. FMM magnitude image of the selected sample area. The circled triangular shape object is believed to be a GO flake.

Figure 5 shows the contact mode topography image of a selected area on the newly synthesized GO-*Loxosceles* silk nanocomposite. The scale bar in the upper-left corner provides a reference of the size of the scanning area. The color bar on the right uses a spectrum of colors to illustrate relative heights, where the zero height point (black) is set as the lowest point on the entire silk surface. In the contact mode topography image, we were unable to observe any GO flakes. This result was expected as the thickness of single layer GO flakes is less than the surface roughness of the *Loxosceles* spider silk.

However, LFM and FMM scans of the same area reveal some features that are unseen in contact mode (Figs. 6–7). In both LFM and FMM, a triangular shape is clearly visible (Figs. 6–7, black circle). The sharp edges and color of the object indicate that it is a GO flake. In the FMM images, the object is brighter than the substrate (silk), implying that the object is stiffer than the *Loxosceles* silk—an expected result.

We then performed a cross-section analysis of the GO flake on the contact topography image,

which suggests that the thickness of the GO flakes is less than 3 nm (Fig. 6). This indicates that the GO flake is a single or double layer flake and explains why we are unable to visualize the flake under contact mode topography images. We conclude that the triangular object is a single-layer or double-layer GO flake, indicating that the spin-coating methods is viable on glass substrate.

It is also worth mentioning that the FMM image has a relatively lower resolution compared to the LFM image. This difference is expected since FMM is generally a more aggressive imaging mode compared to LFM. Additionally, the contrast between GO and silk is greater in the FMM image than in the LFM image.

Natural drying of GO solution

GO was also naturally dried to deposit it on PDMS and imaged in contact mode, LFM, FMM, and FMM phase mode (Figs. 9–15). On the PDMS substrate, the results of LFM and regular FMM tend to be undesirable. The LFM mode generally provides images with little contrast between GO and silk, whereas the FMM mode sometimes produces inconsistent results over the same scanning area. Hence, for both natural drying of GO solution sample and acid-incubation sample, we adopt FMM phase imaging mode as the major imaging mode.

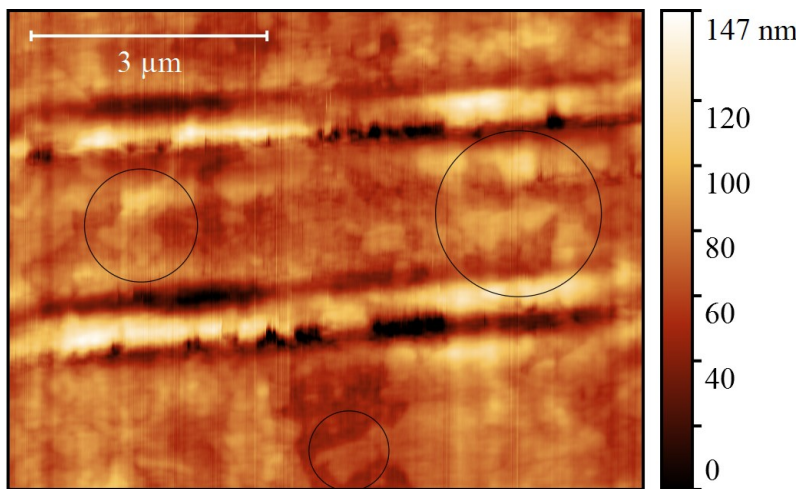


Figure 9. Contact topography mode image of a selected area of the natural drying sample. Circled object are possible GO flakes.

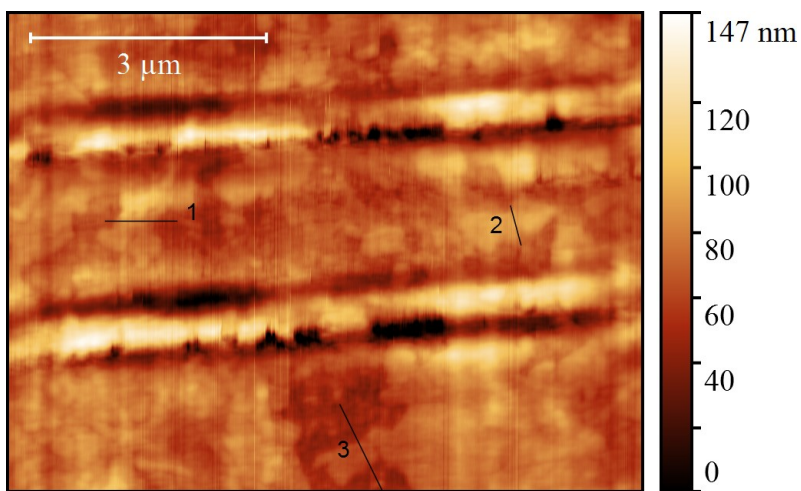


Figure 10. Contact topography mode image of a selected area of the natural drying sample. Cross-sections 1, 2, and 3 correspond to the analysis show in Figure 10, 11, and 12 respectively.

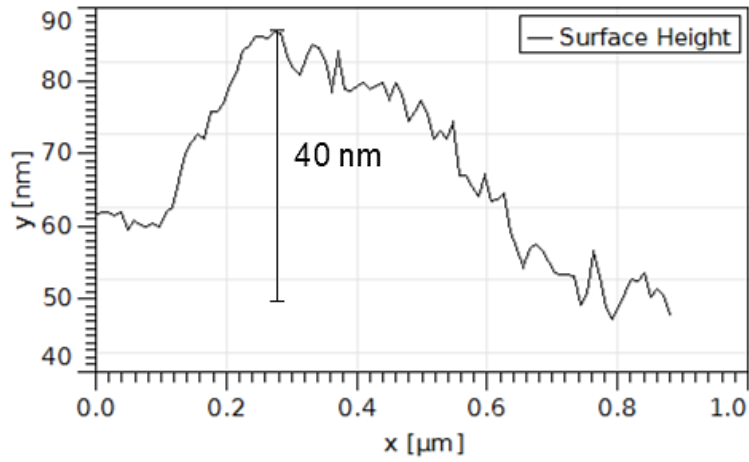


Figure 11. Cross-section analysis of cross-section 1 in Figure 9. The height value is rounded to the nearest tenth.

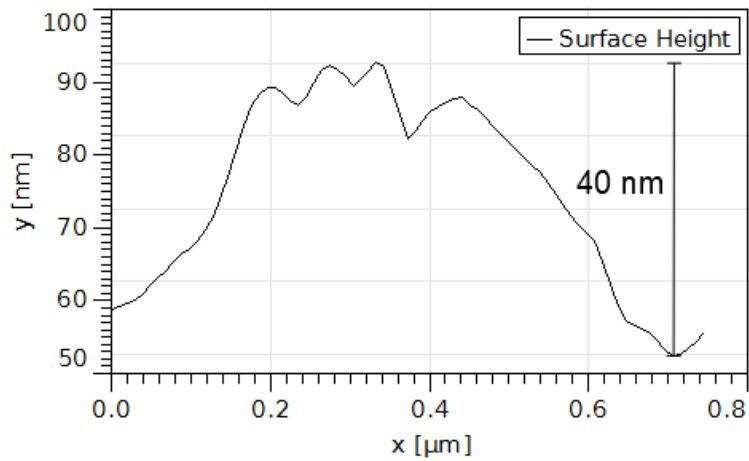


Figure 12. Cross-section analysis of cross-section 2 in Figure 9. The height value is rounded to the nearest tenth.

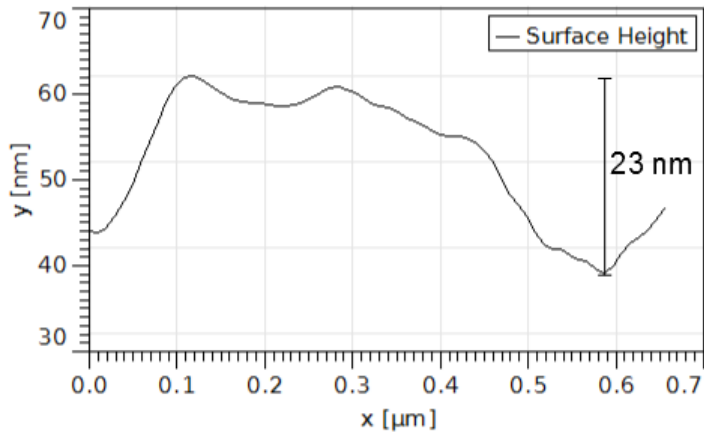


Figure 13. Cross-section analysis of cross-section 3 in Figure 9. The height value is rounded to the nearest whole number.

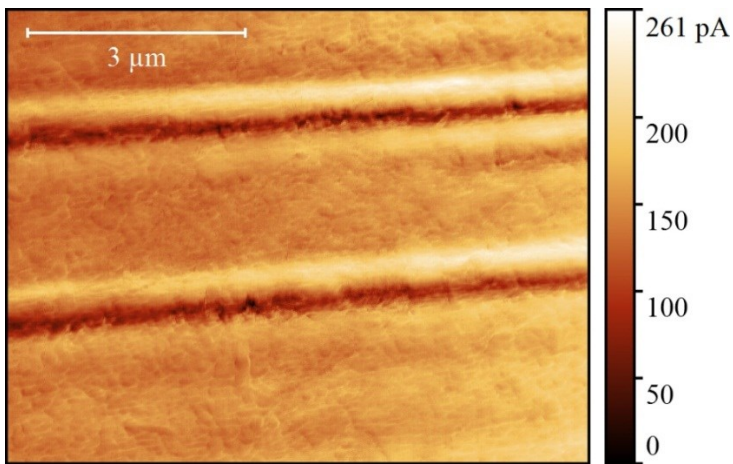


Figure 14. LFM images of the selected sample area on the natural drying sample.

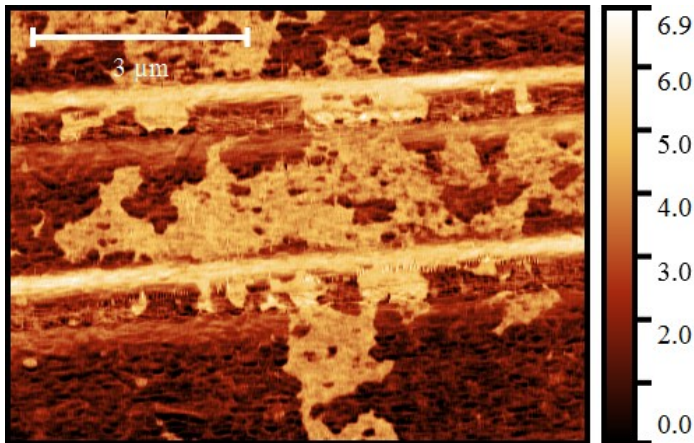


Figure 15. FMM phase image of the selected sample area on the natural drying sample.

In Figure 9 (a contact mode topography image of a selected area on a natural drying sample), we can see a considerable amount of polygonal objects (some of them are circled in Figure 9) which are relatively higher than the substrate silk. The resolution of the image is not high, thus we cannot determine whether these polygonal objects are GO flakes or not from their shape. We then conducted a LFM scan of the sample area (Fig. 14). The LFM image shows very faint contrast, which makes the polygonal objects almost indistinguishable from the silk substrate. A FMM phase mode scan was also conducted after LFM (Fig. 15). Using FMM, we can observe a clear contrast between the polygonal objects (Fig. 15) and the silk. In addition, we believe that the relatively dark regions on the FMM images are GO flakes, which would suggest that the GO flakes stack over the sample surface. This is confirmed by the contact topography cross-section analysis (Figs. 11–13). As shown in the cross-section analysis, the circled polygonal objects have a height ranging from 20 to 40 nm. These values are significantly higher than the thickness of single-layered GO, suggesting that the objects might be a multi-layers of stacking GO flakes. The multi-layer stacking of GO flakes is expected during the natural drying process as a result of the so-called “coffee-ring effect” (15, 16). The coffee-ring effect claims that when a solution droplet dries, capillary flows will induce the solvent to the edge of the droplet ring. After the solvent evaporates out, the solute will be deposited over the edge of the droplet ring

instead of being uniformly deposited over the entire droplet area (Fig. 16). We confirmed that the selected sample area in is close to the edge of the coffee-ring by performing high resolution optical imaging (Figs. 9, 13–15). This suggests that the stacking of GO flakes is possible on the selected sample area.

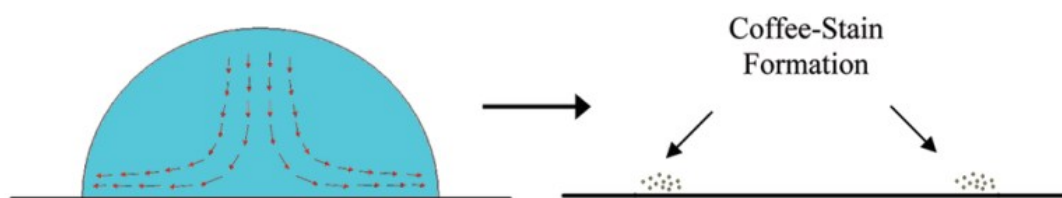


Figure 16. Illustration of the Coffee-ring effect. Adopted from Majumder, et al. Reference 16.

However, since FMM phase images can only distinguish different materials, we are unable to conclude if the polygonal objects are the stiffer material. Therefore, we are unable to determine if they are truly stacks of GO flakes.

Acid-incubation

We then used the acid-incubation technique to deposit GO flakes (Figs. 17–22).

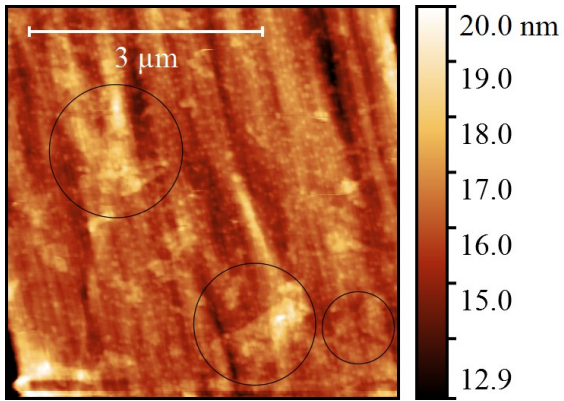


Figure 17. Contact mode topography image of a selected area on the acid-incubation sample. The color bar on the right is adjusted so that the contrast is more noticeable. Circled objects are potential GO flakes.

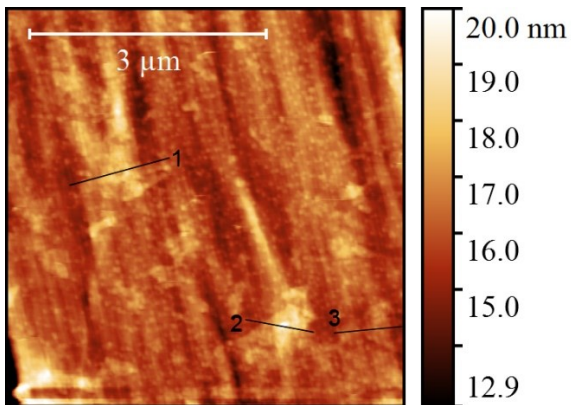


Figure 18. Contact topography mode image of a selected area on acid-incubation sample.

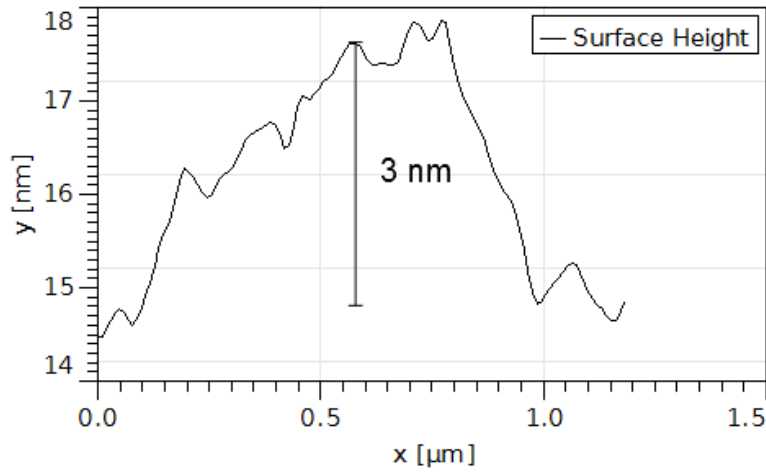


Figure 19. Cross-section analysis of cross-section 1 in Figure 18. The height value is rounded to the nearest whole number.

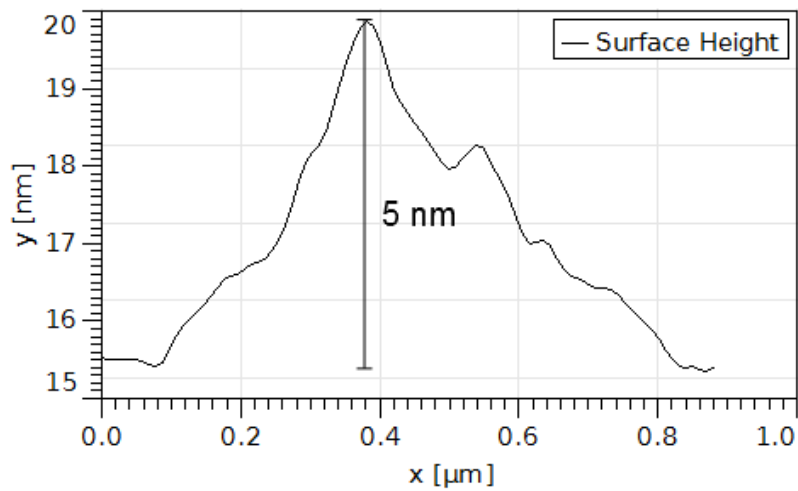


Figure 20. Cross-section analysis of cross-section 2 in Figure 18. The height value is rounded to the nearest whole number.

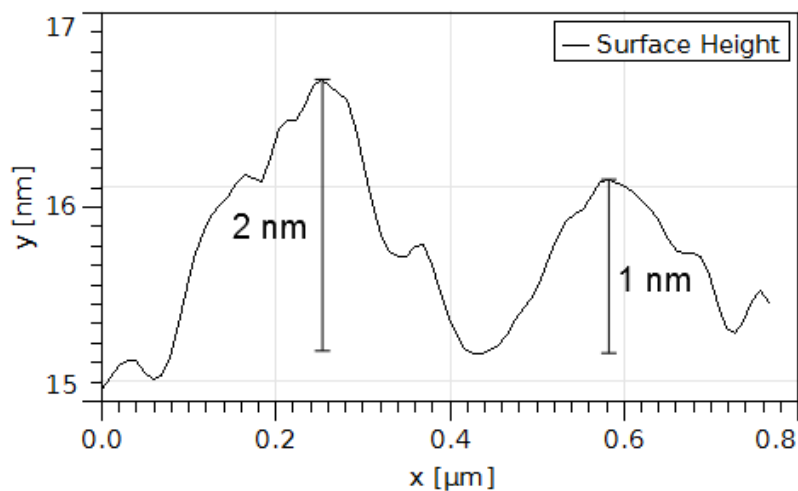


Figure 21. Cross-section analysis of cross-section 3 in Figure 18. The height value is rounded to the nearest whole number.

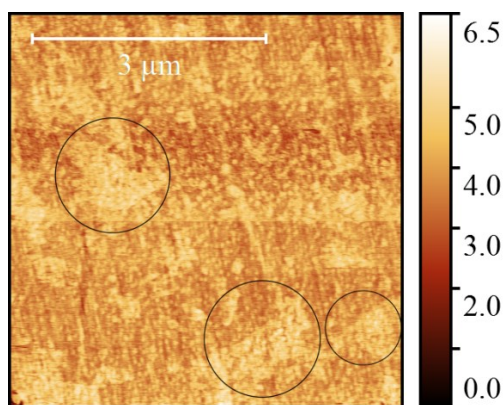


Figure 22. FMM phase image of the selected area on the acid-incubation sample. Circled objects are potential GO flakes.

When the acid-incubation samples were scanned in contact mode (Figs. 17–18), polygonal objects that are higher than the silk substrate were observed. In the FMM phase image, the polygonal objects are also observed. The sharp edges of the polygonal objects suggest they are possibly GO flakes. Cross-section analysis (Figs. 20–22) show that these polygonal objects have heights ranging from 1 to 5 nm, which matches the height of single-layered or double-

layered GO. We can see a contrast between the polygonal objects and the silk most likely because the silk is resting on PDMS. Compared to glass, PDMS is a relatively soft material. During the contact mode scanning, the force created by tip-sample interaction might indent part of silk onto PDMS. Since GO is harder than silk, the indenting effect is less significant on GO than on silk, hence creating a small difference in local height across the silk surface; areas with GO on top would indent less, and thus return a greater height.

However, as with the previous natural drying sample, we have no evidence as to whether the polygonal objects are harder than silk. Therefore, we cannot conclude with certainty that the polygonal objects are GO flakes

Future perspectives

As previously suggested, we do not have enough evidence to suggest that there are GO flakes on the natural drying sample and acid-incubation sample. The next step will be to confirm that the polygonal objects on both samples are GO flakes. Currently, we are investigating the use of Raman spectroscopy to identify GO flakes on silk surface (17).

In addition, the contrast between GO and silk in all of the AFM imaging modes in this project is weak. This makes it difficult to quantitatively analyze the grain size of the GO flakes. We plan to adopt another imaging technique, Ultrasonic Force Microscopy, to solve the imaging problem.

Moreover, we expect to explore the mechanical properties of this novel GO-*Loxosceles* silk. Our lab previously conceived a custom mechanical testing stage for *Loxosceles* spider silk using cover glass. In the future, we plan to use this stage to test the mechanical properties of GO-silk nanocomposite. We would also like to know how well the GO flakes are attached to the silk. To test this, we have designed a stretching stage that will stretch the GO-silk nanocomposite rested on an elastic polymer substrate (our current choice of polymer is PDMS). After each stretch test, we will use the AFM to scan the surface of the nanocomposite and measure the change of grain size of GO, which will indicate how much strain is transferred to

each GO flake by its adhesion to the PDMS.

Conclusion

In this project, we studied three synthesis approaches of a novel GO-*Loxosceles* spider silk nanocomposite—spin-coating method, natural drying of GO solution method, and acid-incubation method. The spin-coating method proved to be feasible. The latter two approaches yielded promising results, but we still lack of enough evidence to suggest that such synthesis methods are viable. To further test the viability of the three methods, characterization techniques such as Raman spectroscopy may be employed.

We also explored the use of three special AFM imaging modes to visualize the novel material: lateral force mode (LFM), force modulation mode (FMM), and FMM phase imaging mode. While the three special modes have generated promising images, we need to enhance the image quality and GO-silk contrast in order to conduct quantitative analysis.

The next step of our project involves testing the mechanical properties of the nanocomposite and the adhesive properties of GO on the *Loxosceles* silk surface. This would provide us with further details about the properties of this novel composite.

Acknowledgements

I would like to thank Sean Koebley, Laura Rickard, Jing Ye, and Qijue Wang for their help and support during this project, and Minzhen Cai for providing me useful data and information in her PhD dissertation. I would also like to thank Prof. David Kranbuehl and Prof. John Poutsma for devoting their precious time to reading my thesis and attending my defense. Lastly, I would like to thank Dr. Hannes Schniepp for his mentoring and advice during this process.

Reference

1. H.C. Schniepp, S.R Koebely, and F. Vollrath. "Brown Recluse Spider's Nanometer Scale Ribbons of Stiff Extensible Silk". *Adv. Mater.* 25 (48): 7028–7032 (2013).
2. D.P. Knights and F. Vollrath. "Spinning an elastic ribbon of spider silk". *Philos Trans R Soc Lond B Biol Sci.* 357(1418):219-27 (2002)
3. V. Dhand, K.Y. Rhee, H.J. Kim, and D.H. Jung. "A Comprehensive Review of Graphene Nanocomposites: Research Status and Trends". *Journal of Nanomaterials.* 2013, Article ID 763953: 14 pages (2013)
4. R.J. Young, I.A. Kinloch, L Gong, K. S. Novoselov. "The mechanics of graphene nanocomposites: A review". *Composites Science and Technology* 72: 1459–1476 (2012)
5. J. R. Potts, D.R. Dreyer, C.W. Bielawski, R.S. Ruoff. "Graphene-based polymer nanocomposites". *Polymer* 52: 5-25 (2012).
6. S.Wang, Y. Zhang, N. Abidi, and L. Cabrales. "Wettability and Surface Free Energy of Graphene Films". *Langmuir.* 25 (18): 11078–11081 (2009).
7. W. Zheng, B. Shen and W. Zhai. "Surface Functionalization of Graphene with Polymers for Enhanced Properties". *New progress in graphene research. Chaper8. InTech.* ISBN: 978-953-51-1091-0.

8. W.C. Hou, I Chowdhury, D. G. Goodwin, J. W. M. Henderson, D. H. Fairbrother, D Bouchard, and R. G. Zepp. Photochemical Transformation of Graphene Oxide in Sunlight. *Environ. Sci. Technol*, 49(6):3435–3443 (2015).
9. G Altankov, and T Groth. “Reorganization of substratum-bound fibronectin on hydrophilic and hydrophobic materials is related to biocompatibility” *Journal of Materials Science: Materials in Medicine*. 5 (9-10): 732-737 (1994).
10. D Bodas, and C.Khan-Malek. “Hydrophilization and hydrophobic recovery of PDMS by oxygen plasma and chemical treatment—An SEM investigation”. *Sensors and Actuators B*. 123: 368–373 (2009)
11. C. J. Lawrence. “The mechanics of spin coating of polymer films”. *Physics of Fluids*. 31: 2786 (1988).
12. T Dyakonov, C.H. Yang, D Bush, S Gosangari, S Majuru, and A Fatmi. “Design and Characterization of a Silk-Fibroin-Based Drug Delivery Platform Using Naproxen as a Model Drug”. *Journal of Drug Delivery*. 12, Article ID 490514: 10 pages.
13. P Eaton and P West. *Atomic Force Microscopy*. Atomic Force Microcopy. Oxford Press. ISBN:978-0199570454
14. M Cai. *Nanoscale Mechanical Characterization of Graphene/Polymer Nanocomposites*

using Atomic Force Microscopy. PhD Dissertation. College of William and Mary (2012).

15. R.D. Deegan, O Bakajin*, T.F. Dupont, G Huber, S.R. Nagel, and T.A. Witten.

“Capillary flow as the cause of ring stains from dried liquid drops”. *Nature*. 389: 827-829 (1997).

16. M Majumder, C.S. Rendall, J. A. Eukel, J.Y.L. Wang, N Behabtu, C.L. Pint, T. Liu, A.W. Orbaek, F Mirri, J Nam, A.R. Barron, R.H. Hauge, H.K. Schmidt, and M Pasquali.

“Overcoming the “Coffee-Stain” Effect by Compositional Marangoni-Flow-Assisted Drop-Drying”. *J. Phys. Chem. B*. 116 (22): 6536–6542 (2012).

17. H.J. Kim, S Lee, Y Oh, Y Yang, Y Li, D.H. Yoon, C Lee, J Kim, and R.S. Ruoff.

“Unoxidized Graphene/Alumina Nanocomposite: Fracture- and Wear-Resistance Effects of Graphene on Alumina Matrix”. *Scientific Reports*. 4:5176 (2014).